Published in final edited form as:
Curr Drug Metab. 2010 July ; 11(6): 483–493.

Applications of LC-MS in PET Radioligand Development and Metabolic Elucidation

Ying Ma, **Dale O. Kiesewetter***, **Lixin Lang**, **Dongyu Gu**, and **Xiaoyuan Chen***
Laboratory of Molecular Imaging and Nanomedicine (LOMIN), National Institute of Biomedical Imaging and Bioengineering (NIBIB), National Institutes of Health (NIH), Bethesda, MD 20892, USA

Abstract

Positron emission tomography (PET) is a very sensitive molecular imaging technique that when employed with an appropriate radioligand has the ability to quantititate physiological processes in a non-invasive manner. Since the imaging technique detects all radioactive emissions in the field of view, the presence and biological activity of radiolabeled metabolites must be determined for each radioligand in order to validate the utility of the radiotracer for measuring the desired physiological process. Thus, the identification of metabolic profiles of radiolabeled compounds is an important aspect of design, development, and validation of new radiopharmaceuticals and their applications in drug development and molecular imaging. Metabolite identification for different chemical classes of radiopharmaceuticals allows rational design to minimize the formation and accumulation of metabolites in the target tissue, either through enhanced excretion or minimized metabolism. This review will discuss methods for identifying and quantitating metabolites during the pre-clinical development of radiopharmaceuticals with special emphasis on the application of LC/MS.

Keywords

Positron emission tomography (PET); Radiopharmaceutical; LC/MS/MS; Metabolite

INTRODUCTION

Positron emission tomography (PET) is the most sensitive external imaging technique in the molecular imaging arsenal that can be applied to living patients [1, 2]. The technique images the co-linear annihilation photons resulting from decay of positron-emitting radionuclides. Positron-emitting radionuclides most commonly introduced into molecules for PET are C-11 ($t_{½}$ 20.4 min), and F-18 ($t_{½}$ 119.8 min). Other radionuclide used in some research centers are Br-76 ($t_{½}$ 16.2 h), Cu-64 $t_{½}$ 12.7 h), Ga-68 ($t_{½}$ 68 min), and I-124 ($t_{½}$ 4.18 d). The short half-lives of the more commonly used C-11 and F-18 create challenges to their application in PET. The first challenge is the need to incorporate the radionuclide into more complicated chemical structures. The short half-lives require that the incorporation be performed as close to the final synthetic step as possible. The second major challenge is completing a radio-chemical synthesis, purification, and conducting pharmacokinetic imaging studies before the decay of the radionuclide affects the radioactive counting statistics.

*Address correspondence to these authors at the 31 Center Dr, Suite 1C14, NIBIB/NIH, Bethesda, MD 20892-2281; USA; Tel:/Fax: 301-451-4246; shawn.chen@nih.gov; and 10 Center Drive MSC 1180, NIBIB/NIH, Bethesda, MD 20892; USA; Tel/Fax: 301-451-3531; dk7k@nih.gov.

The true power of the PET technique can be exploited by attaching these positron-emitting radionuclides to molecules that have high affinity to biological targets or participate in specific biological transformations (i.e. the specific phosphorylation of 2-[^{18}F]fluorodeoxy-glucose that results in accumulation of radioactive emission from cells that take up high quantities of glucose [3]). However, the PET scanner detects only coincident photons; there is no information concerning the chemical structure to which the radionuclide is attached. In order to validate a new radioligand for its intended target, assurance that the radioactive emissions derive primarily from the parent radioligand is required. Knowledge of metabolic rate and the structure of radiolabeled metabolites can allow prediction of the propensity of the metabolites to confound image interpretation [4, 5]. Therefore, identification of metabolic profiles of labeled compounds is an important aspect of design, development, and validation of new radiopharmaceuticals.

The metabolism profile of a potential radioligand in mice or rats is important for all of the preclinical validation studies for the purpose of determining specificity or selectivity for the target. However, the fact that metabolism may be very different in humans requires some method for assessing species differences [6]. The rodent may turn out to be a very poor model on which to base preclinical studies. This review will focus on methods of metabolite identification, species differences of metabolic profiles, and the application of high performance liquid chromatography/mass spectrometry (LC/MS) in the preclinical design and evaluation of novel radiopharmaceuticals.

METABOLITE IDENTIFICATION

The pharmaceutical industry expends a great deal of effort to identify metabolites of its drug candidates in order to understand absorption, distribution, metabolism, excretion, and toxicity (AD-MET) [7]. Identification of metabolites allows rational pharmaceutical design to minimize formation of undesirable metabolites that may affect drug safety. In addition, knowledge of the metabolite structure may allow a study of the contribution of pharmacologically active or toxic metabolites to the overall pharmacological response. The pharmaceutical industry integrated LC/MS into its drug discovery process several years ago [8]. Identification of metabolites of radiopharmaceuticals, which is complicated by the short half-lives of the radionuclides and the very low dose of the compound [typically less than 10 nmol] administered, may provide suggestions as to the most appropriate position in the molecule to attach the radiolabel and allow the synthesis and study of the bio-distribution of the metabolite(s) [9, 10].

Quantitative whole-body autoradiography (QWBA) [11] and MS imaging [12, 13] have been used to evaluate drug concentrations ex vivo. QWBA relies on the preparation of images showing the distribution of radioactivity in the whole body. Although the parent drug may constitute some of the radioactivity measured, it is probable that radiolabeled metabolites will also be present in an unknown amount. The separation and evaluation of mixtures of parent compound and metabolites can only be performed by other analytical methods. MS imaging has the potential to deliver highly parallel, multiplexed data on the specific localization of parent and metabolites in tissue samples directly, and to measure and map the variations of these ions during development and disease progression or treatment. However, the sensitivity of MALDI –MSI, even with the recently introduced nanostructure initiator mass spectrometry (NIMS), make it challenging to analyze radiopharmaceuticals and their metabolites at the radiotracer level.

Although pharmacokinetic analysis of radiotracers can be conducted even if more than one chemical entity is observed in the target tissue, the analysis is much simpler when only parent radioligand is present. The time dependent concentration and the relative biological

activity (receptor affinity or rate of enzymatic conversion) of each radiolabeled component must be known. Usually this information is unknown and thus the presence of metabolites in the tissue of interest is a major reason for discontinuing further studies of new ligands [14].

Normal metabolic processes on small drug-like molecules (MW < 1000) usually results in the generation of more polar species. The blood brain barrier (BBB) generally prohibits more polar metabolites from crossing into the brain. Traditionally, the observation of metabolites that cross the BBB results in a search for a new position to insert the radionuclide or the radioligand is discarded for a different chemical class. The traditional method for evaluating metabolites in the brain was to extract rat or mouse brain tissue and evaluate the radioactive components by thin layer chromatography (TLC) or HPLC. With the increasing application of PET to targets outside the brain, this natural restriction provided by the BBB has been lost.

The inherent inability of PET to differentiate between a parent compound and its metabolites confounds the interpretation of images and may impact the identification of the pathologically induced biochemical changes under investigation. Cytochrome P450 isoforms play a major role in mammalian xenobiotic biotransformation [15]. The utility of liver hepatocytes to generate phase 1 (i.e. oxidation by cytochrome P450) and phase 2 metabolites (i.e. glucuronidation of hydroxyl groups) of proposed radioligands followed by the analysis of the metabolites has been exploited to determine metabolic pathways [4, 16, 17]. The use of liver microsomes, which produce predominately first order metabolites, has also been used extensively [18]. Hepatocytes obtained from Sprague-Dawley rats give fairly consistent results from lot to lot because of the homogeneous genetic makeup of these animals. Human hepatocytes, on the other hand, are somewhat more variable between lots. More recently, commercial vendors of these products are providing hepatocytes that are pooled from 10–50 individual samples; which provides more consistent results. Once these cells have been used to generate a metabolism profile, LC/MS can be applied to identify the possible structures and quantitate the metabolism rate of the parent radioligand.

LC/MS has the unique combination of sensitivity and mass selectivity to provide sensitive detection and mass to charge ratio (m/z) data that can be used to propose metabolite structure [7]. In addition, the ability to conduct LC/MS/MS studies provides even greater power for assignment of possible structure. The various m/z components from collision induced fragmentation of the parent ion can provide information on the structure of the parent ion. Multiple reaction monitoring (MRM) is an LC/MS/MS technique that allows scanning for several daughter ions from a single parent ion. Since many metabolites derive from oxidation, some fragment peaks of metabolites may be the same as the parent. Thus metabolites may be detected and identified based on observation of the daughter ions from the parent.

The combination of two general classes of experiments, metabolite generation with hepatocytes from various species and LC/MS techniques, provides a general approach to predict the rate of metabolism, predict species differences, and assign chemical structures to metabolites. The structural identity of metabolites can be utilized to direct the design of improved radioligands with a new metabolic profile that improves the utility as an imaging agent. The extreme sensitivity of LC/MS can allow *in vivo* biodistribution studies of non-radiolabeled compounds at very low mass doses. In the following sections, we will discuss specific examples that illustrate the application of these techniques to preclinical studies with PET radioligands.

Muscarinic Receptor Ligands

The muscarinic receptor partial agonist 3-(3-(3-fluoropropyl) thio)-1,2,5-thiadiazol-4-yl-1,2,5,6-tetrahydro-1-methylpyridine (FP-TZTP) [19-23] is a potential tracer for evaluating M2 muscarinic receptor concentration as a function of Alzheimer's disease. An accurate plasma input function was required for the compartment modeling for analysis of this M2 receptor binding radiotracer, because there is no region in the brain with low or zero concentration of M2 receptor that could be used as a reference region.

We incubated cultured rat hepatocytes with [^{18}F]FP-TZTP [24]. The time course of metabolite formation from the time dependent analysis of the no-carrier-added [^{18}F]FP-TZTP revealed that the radiolabeled parent compound was nearly consumed within 2 h, concomitant with the formation of radiolabeled metabolites based on radiochemical detection Fig. (1). The experiment was repeated with the addition of carrier FP-TZTP to provide additional mass to more easily identify the metabolites by LC/MS Fig. (2). Two of the compounds showed a mass increase of 16 from the parent ligand. This is consistent with oxidation of nitrogen (Met-1) or sulfur (Met-2). Another metabolite showed a mass decrease of 14, consistent with N-demethylation (Met-3). Another metabolite showed a mass decrease of 4, which can be rationalized as oxidation of the N-methyl tetrahydropyridine ring into an N-methylpyridinium structure (Met-4). One metabolite showed a mass increase of 15 over the metabolite Met-4, and can be rationalized as the cyclic amide Met-5. For four of these metabolites, Met-1, Met-2, Met-3, and Met-4, the structures were confirmed by comparison of retention time and LC/MS/MS fragmentation with chemically synthesized authentic standards. This observed metabolic profile was very similar in human hepatocytes [24].

Mass spectral detection is usually not quantitative among different structures as the mass spectral response is compound specific. We relied on the HPLC radiochromatogram for quantitation with an on-line radio detector between UV and MS. N-oxidation (Met-1) was the major radioactive metabolite. In addition to these major metabolites of FP-TZTP identified above, two more polar radioactivity peaks were found in the radiochromatogram. The peak eluting at the solvent front was assigned as [^{18}F]fluoride based on co-elution with authentic [^{18}F]fluoride. The remaining peak which eluted just after fluoride (Fig. (2)) was not identified as we could not arrive at a structural assignment based on the LC/MS/MS data.

We observed that the rat metabolite profile *in vivo* of plasma extracted radioactivity was similar to that found with hepatocytes *in vitro*. As previously stated, the imaging application of [^{18}F]FP-TZTP required a plasma input function corrected for the parent concentration in human. Since we knew the identification of the metabolites, we developed a two-step liquid-liquid extraction procedure that allowed quantification of parent [^{18}F]FP-TZTP concentration in plasma [25]. The plasma was added to KCl-NaOH buffer followed by extraction with organic solvent (Hexane:EtOAc = 4:1). After mixing, the layers were separated by centrifugation. The aqueous phase was frozen in dry ice; the organic phase was collected and treated with acetic anhydride. The organic fraction was extracted with 0.1 M HCl. The aqueous phase contained unmetabolized parent compound. After the first extraction step, the organic soluble material contains both [^{18}F]FP-TZTP and the demethylated metabolite (Met-3), while the N-oxide metabolite (Met-1), Met-4, and Met-2 remained in the aqueous layer Fig. (3a). Acetylation of the secondary amine of Met-3, by treating the organic extract with acetic anhydride, formed an amide and allowed extraction of the parent in acidic aqueous media Fig. (3b). When using pure parent [^{18}F]FP-TZTP, the total extraction efficiency of parent in this study for the two extraction steps was 92.0 ± 2.8%.

We also analyzed a second compound, an [^{18}F] analogue of xanomeline [26] in this thiadiazole series of muscarinic ligands, one that possesses some selectivity for M1. This compound differs structurally from FP-TZTP in that it lacks the side chain sulfur and has a longer alkyl chain. Similar to [^{18}F]FP-TZTP, the major metabolite of [^{18}F]xanomeline was identified as the N-oxide, consistent with our observations with FP-TZTP and with literature from the group at Eli Lilly [27, 28] Fig. (4). Since [^{18}F]xanomeline lacks the sulfur atom, the sulfoxide metabolite was avoided. The other metabolites were also consistent with our results from FP-TZTP, demethylation of the tertiary amine, dehydrogenation of the tetra-hydropyridine ring, and its oxidation product, respectively. Rat, monkey and human hepatocytes produced a similar metabolite profile. We also compared the metabolism rate in hepatocytes of the three species using LC/MS and radio-chromatography and found that the relative metabolism rate is monkey > rat > human [26].

Serotonin 5HT$_{1A}$ Receptor Ligand Compounds

In contrast to FP-TZTP, the class of serotonin compounds based onWAY100635 (N-(2-(1-(4-(2-methoxyphenyl)piperazinyl)ethyl))-N-(2-pyridinyl)cyclohexanecarboxamide) Fig. (5) demonstrated a significant species difference. This example demonstrates the utility of metabolite information to guide radioligand design. WAY-100635 was developed as a radioligand for static measurement of 5-HT$_{1A}$ receptor distribution in the human brain utilizing PET in patients with psychiatric and neurological disorders, such as anxiety, depression, and Alzheimer's disease [29]. This compound was first radiolabeled with an ^{11}C methyl group on the phenolic methyl position [30]. A radiometabolite was observed in the brain and identified as WAY100634 [31, 32], which was the result of amide hydrolysis. This radiolabeled metabolite was problematic in that it displayed specific receptor mediated uptake as well as non-specific uptake. With the knowledge of this metabolite formation, the radiolabel was moved into the cyclohexanecarboxylate portion of the structure with the expectation that the radiolabeled metabolite would be a polar carboxylic acid. Amide hydrolysis by metabolic enzymes, presumably located in liver, formed [^{11}C]cyclohexane-carboxylic acid as the primary radiometabolite, which gained only transient and low access to brain [31]. The location of the radiolabel in the carboxyl carbonyl resulted in a much improved carbon-11 labeled radiopharmaceutical. In an effort to reduce the amide hydrolysis, one research group has reported preparing more hindered amide groups than cyclohexanecarboxamide [33]. Another analogous radioligand, (R)-[^{11}C]RWAY [14], was developed that displays an amide that resisted enzymatic hydrolysis. (R)[^{11}C]RWAY gave blood and urine radiometabolites that were less lipophilic than the parent molecule [34–36].

We developed [^{18}F]fluorine analogues of WAY100635 in order to evaluate the potential benefits of the longer-lived radionuclide and to evaluate the use of ligands with slightly lower affinity and slower pharmacokinetics that may be sensitive to endogenous ligand concentration. Placing the fluorine in the cyclohexane ring resulted in formation of different isomers. We examined the relationship between structure and metabolism [9, 10, 37, 38]. The first four compounds, prepared both chemically and radiochemically, were 4-*cis*, 4-*trans*, 3-*cis*, and 3-*trans* isomers of *N*-{2-[4-(2-metho-xyphenyl)piperazinyl]ethyl}-*N*-(pyridin-2-yl) -fluorocyclohexane-carboxamides (FCWAY's) Fig. (5) [10]. The higher affinity 4-*trans*-[^{18}F]FCWAY was most promising for measuring receptor density given its high hippocampus to cerebellum ratio in rat, whereas 3-cis-[^{18}F]FCWAY could be sensitive to competition by endogenous serotonin ligand due to the lower affinity and faster clearance from the brain [9].

The *in vitro* hepatocyte metabolism of 4-*trans*-FCWAY revealed a very complex mixture of metabolites Fig. (6) [39]. Both rat and human species showed common pathways of oxidation, de-fluorination, and dealkylation. In addition, human hepatocytes showed amide hydrolysis. Oxidation with formation of a phenol was the major metabolic pathway for rat

hepatocytes and amide hydrolysis was the major metabolic pathway for human hepatocytes. The position of the oxidation was suggested based on LC/MS/MS. The phenolic metabolite was identified based on the fact that the daughter ion containing the anisole ring had an increase of 16 mass units compared to the daughter ion of parent FCWAY. It is important to point out that many of the metabolites no longer contain fluorine. For imaging purposes, only radiolabeled metabolites are of concern.

The 4-*trans*-[^{18}F]FCWAY was studied extensively by us in rhesus monkeys and eventually applied to human studies. The metabolite 4-*trans*-fluorocyclohexane carboxylic acid was found to have a very low uptake into the brain, but uptake sufficient that correction of the PET data for its presence in the brain improved the statistical fit to the pharmacokinetic model [37]. Metabolic de-fluorination of [^{18}F] fluoride was not insignificant and presented no problems in PET data interpretation in the rhesus monkey. However in human, the higher amount of defluorination, probably due to the higher amount of amide hydrolysis, coupled with a thicker skull caused spill-over of radioactive counts into the brain from the skull uptake. This created difficulties in interpretation of PET data when the brain region of interest was located near the skull (i.e. cortex) but not with brain regions farther from the skull. We utilized our knowledge of the structure of the metabolites to develop a procedure to extract parent FCWAY into 20% ethyl acetate in hexane from pH 12.5 buffer, leaving the major radiolabeled metabolites, 4-fluoro-cyclohexanecarboxylic acid and the phenol in the aqueous phase layer Fig. (7) [25]. Therefore, we can determine parent concentration in plasma using a single extraction by counting the radioactivity of organic phase which contained only parent compound. The parent fraction obtained from this extraction procedure was used to generate the metabolite corrected plasma input function for analyzing PET imaging data according to mathematical models [33, 40].

The extraction procedure has advantages over chromatography for the parent concentration because of its simplicity and speed. The expectation is that clinical plasma samples may not contain sufficient mass for detection and quantification. For quantitative analysis, radioactivity is the more sensitive detection method. HPLC flow radioactivity detectors are typically not sensitive enough for plasma extract samples, particularly at late time points following injection. Thus, radioactivity counting requires the use of a gamma counter and the parent radioligand quantification will require an efficient separation from radiolabeled metabolites. Standard analytical HPLC separation and fraction collection was necessary prior to gamma counting. The validated extraction procedure allows more samples to be processed and counted compared with standard HPLC during the short half-life of F-18 and C-11 radioisotopes. With continued improvements in HPLC/MS sensitivity, this technique may eventually prove superior to extraction.

We further evaluated the metabolism of 3-*cis* and 3-*trans*-FCWAY in rat, monkey and human hepatocytes and obtained similar profiles and species differences as observed with 4-*trans*-FCWAY [6]. The metabolism of this class of compounds undergoes a transition from aromatic oxidation to amide hydrolysis as the major metabolic pathway as one progresses up the species ladder from rat to human. In human, hydrolysis of the amide linkage was the major metabolic pathway. In monkey, both pathways (oxidation and amide hydrolysis) were observed.

We also examined 4-fluorobenzamide analogues, FBWAY, FPWAY, and MeFBWAY Fig. (5), because arylfluorides tend to resist defluorination [41]. These *in vitro* metabolism studies indicated that hydrolysis of the amide linkage was the major metabolic pathway for FPWAY and FBWAY in human hepatocytes, whereas aromatic oxidation is the major metabolic pathway for MeFBWAY. The unique metabolite that was observed in these compounds was O-demethylation of the aromatic methoxy moiety. The comparative

metabolic rate, measured by decrease in parent compound, in human hepatocytes was FPWAY > FBWAY > MeFBWAY. In rat hepatocytes, aromatic oxidation was the major metabolic pathway for all three analogs and the rate was similar for all of the analogues.

In rat, monkey and human hepatocyte assays, the relative rate of defluorination was 4-*trans* = 4-*cis* ≈ 3-*trans* ≫ 3-*cis*-FCWAY ≈ FBWAY. This result corresponds well with *in vivo* bone uptake studies. Based on our results with this short series of WAY analogues, defluorination seems to correspond to the amount of amide hydrolysis leading us to hypothesize that defluorination proceeds from the fluorocyclohexane carboxylic acid. The low defluorination of the aromatic acids was expected based on previous literature and the low defluorination of *cis*-3-fluoro was not predicted.

In order to demonstrate the potential for metabolite quantification of FPWAY *in vivo*, we analyzed plasma and brain tissue extracts following i.v. administration to rats using a MRM mass scanning procedure. The plasma extracts obtained at 30 min exhibited mass spectral signals consistent with parent compound (A), oxidation (B), amide hydrolysis metabolites (C), and demethylation (D) (Fig. (8)) as expected from our previous metabolism study. In this same experiment, extracts of the rat brain presented mass spectral signals consistent with parent FPWAY, oxidation, and demethylation metabolites.

Radiolabeled Paclitaxel

Paclitaxel (PAC) is a complex diterpene natural product that has application as a chemotherapeutic agent in a number of solid tumors [42]. However, the P-glycoprotein (P-gp) efflux pump reduces the effectiveness of paclitaxel in treating some tumors. Measurement of the *in vivo* concentration of a positron-emitting PAC derivative in tumors could non-invasively predict, prior to chemotherapy, therapeutic efficacy. The derivative [^{18}F]-Paclitaxel ([^{18}F]FPAC) was sensitive to the presence or absence of P-gp in knockout mice and sensitive to administration of XR9576, a P-gp modulator in monkeys [43, 44].

Metabolism studies of [^{18}F]FPAC, [^{76}Br]BPAC and [^{124}I]IPAC were conducted using cryopreserved hepatocytes from rat and human tissue. In human hepatocytes, [^{18}F]FPAC parent compound represented approximately 50% of the radioactivity after 4 h. A single radioactive metabolite was observed that represented the remainder of the radioactivity. This metabolite is believed to be the known 6-hydroxy paclitaxel analog by analysis of daughter ions by HPLC/MS/MS. [^{76}Br]BPAC and [^{124}I]IPAC showed the same profile with a single metabolite that is also consistent with hydroxylation. The $t_{1/2}$ for parent compound was 172, 408, and 547 min for [^{18}F]FPAC, [^{76}Br]BPAC, and [^{124}I]IPAC, respectively.

In rat hepatocytes, three metabolites were observed for each of the radioligands (Fig. (9)). The major metabolite, in the case of FPAC was identified as N-(4-fluorobenzoyl) phenylisoserine (4), product of hydrolysis of the C-13 ester of paclitaxel. The other metabolites were the products of hydroxylation (2) and de-acylation (3). The rates of metabolism were similar for [^{76}Br]BPAC and [^{124}I]IPAC, with calculated $t_{1/2}$ values of 277 and 270 min, respectively. The fluoro analogue was metabolized more rapidly, as observed in human hepatocytes, with a $t_{1/2}$ of 194 min.

Radiometal Complexes of Azamacrocycles

Radiometals are of significant interest for PET radiochemistry; they exhibit a variety of half-lives and positron energies that are complimentary to the more common radioisotopes. Labeling with metals requires the use of a bifunctional chelating group that provides for attachment to biological targeting molecules and chelation of the metals. The azamacrocycles are very often used as chelators for radiometals such as Cu-64 as they provide highly stable complexes. The stability of the metal chelate *in vivo* is of high

importance as the exchange of the metal leads to background radioactivity emissions in an analogous fashion to the metabolic loss of F-18 that has been described above.

An LC-MS methodology for separation and characterization of radiometal-labeled complexes would be advantageous because of the requirement of high sensitivity for detection and characterization of these radiometal complexes at or near the tracer level [45]. Incorporation of the metal into the desired ligand may be confirmed by comparing the retention times of radiolabeled species with the appropriately characterized natural metal complexes confirmed by LC-MS. This radio-LC-MS approach was used to confirm the identities of ^{99m}Tc-Sestamibi [46] and other ^{99m}Tc radiopharmaceuticals [47, 48], a process that is usually achieved at the tracer level only indirectly by assessment of RP-HPLC retention times. Boswell *et al.* [45] described the confirmation of the formation of desired ^{64}Cu-azamacrocyclic complexes at the tracer level, identification of ^{64}Cu-labeled impurities, and investigation of the extent of ^{64}Cu-azamacrocyclic complex metabolism *in vivo*.

The metabolic fates of the ^{64}Cu-labeled azamacrocycles Fig. (10) were investigated by analysis of samples extracted following *in vivo* administration to rats. This was accomplished by analysis of liver extracts obtained from rats at 4 h following intravenous injection of highly concentrated (5 mg/mL) carrier-added ^{64}Cu-CB-TE2A (4,11-bis(carboxymethyl)-1,4,8,1-tetraazabicyclo[6.6.2] hexadcane) or ^{64}Cu-TETA (1,4,8,11-tetraazacyclotetradecane-1,4,8,11-tetraacetic acid). The liver extracts were analyzed by radio-HPLC-MS. Because the HPLC elution times of ^{64}Cu-TETA and ^{64}Cu-CB-TE2A were extremely sensitive to the concentration of the injection, LC/MS was essential in identifying the chemical species eluting with the radioactivity. The resulting radioactivity and LC/MS chromatograms indicated that ^{64}Cu-TETA was metabolized to a significant extent in rat liver while a significant proportion of ^{64}Cu-CB-TE2A remained intact.

The Use of LC/MS to Evaluate Biodistribution

The value of LC-MS as a complementary research tool to evaluate the primary biodistribution of PET radiotracers has been demonstrated. The extremely high sensitivity of newly developed LC/MS equipment allowed quantitative determination of the distribution of radiopharmaceuticals in target tissue at injected masses similar to the radiotracer level [49]. Because LC/MS analyzes the stable nuclides, samples could be stored and used to conduct metabolite assays at a later time; this is not possible using radiodetection of short-lived PET radionuclides. In addition, analyses may be conducted multiple times with the same sample to provide more precision and accuracy. High sensitivity and high resolution LC/MS instrumentation has been applied in PET radiopharmaceutical development to provide quantitative measurement of the mass of radiotracers extracted from tissues of rats [50, 51].

We employed the highly sensitive Waters Q-TOF premier MS coupled with an Acquity UPLC system to demonstrate that LC-MS can generate *ex vivo* biodistribution data for the 5-HT_{1A} PET ligand FPWAY without the need to radiolabel[45]. Quantitative measurement of parent compound concentration in various tissues by LC-MS, following an administered mass dose of 1 nmol/250 g rat, was compared with quantitative data obtained by gamma counting of co-injected radioactive [^{18}F]FPWAY (0.5–1 mCi/250 g rat, specific acitivity). The six regions of rat brain [hippocampus (Hp), cortex (Cx), cerebellum (Cb), caudate (Cd), brain stem (BS), and thalamus (Th)] and plasma (P) were processed for quantitative measurement of parent compound concentration by LC-MS. The data were converted to (A) the differential uptake ratio DUR (%ID/g × body weight/100) and (B) the brain tissue-specific binding ratio [($DUR_{tissue}/DUR_{cerebellum}$) − 1] to allow direct comparison with data obtained by gamma counting of the coinjected radioactive [^{18}F]FPWAY Fig. (11). The

cerebellum had the lowest uptake because it has no 5-HT_{1A} receptor, therefore cerebellum served as the reference tissue for specific binding. The brain tissue specific uptake ratios and binding ratio determined by the two methods differed by less than 20% and was determined to be not significant [paired t-test, $p>0.05$]. The differential uptake ratio (DUR) and the brain tissue specific binding ratio calculated using the LC-MS method showed a high degree of correlation with the values obtained by standard radioactivity measurements of co-injected [^{18}F]FPWAY. This concordance demonstrates the high sensitivity of LC/MS and validates LC/MS as a new tool for evaluating biodistribution of potential new molecular imaging probes.

CONCLUSIONS

The development of radiopharmaceuticals for PET is complicated by the short half-lives of the radionuclides, the very low dose administered to animals for *in vivo* imaging, and the complex sample matrices provided by tissue extraction. Because LC/MS is generally more sensitive than UV detection and more selective than online γ-radioactivity detection, the technique has been employed in the evaluation of PET radiopharmaceuticals. Hepatocytes from various species were used to generate metabolites of PET radiotracers and LC/MS was employed to analyze the resulting mixtures. LC/MS data can be used to probe species variations in both the identity of metabolites and the rate of metabolism. The combination of LC and MS/MS can provide both structural information for identification of metabolites and high selectivity for accurate quantitation. Knowledge of the metabolites' structures can be used to design radiotracers that have improved properties with respect to stability and biodistribution. Finally, analysis of *in vitro* hepatocyte incubations with LC/MS provides an efficient and sensitive method for screening radiotracer candidates without the need for radiolabeling.

Acknowledgments

Financial support for this work was provided by the intramural program of the National Institute of Biomedical Imaging and Bio-engineering (NIBIB), a component of the National Institutes of Health (NIH), U.S.A.

ABBREVIATIONS

PET	Positron emission tomography
LC/MS	Liquid chromatography/mass spectrometry
ADMET	Absorption, distribution, metabolism, excretion, and toxicity
QWBA	Quantitative whole-body autoradiography
NIMS	Nanostructure initiator mass spectrometry
MALDI MSI	Matrix-assisted laser desorption/ionization mass spectrometric imaging
MRM	Multiple reaction monitoring
BBB	Blood brain barrier
DUR	Differential uptake ratio
TLC	Thin layer chromatography
FP-TZTP	3-(3-(3-fluoropropyl)thio)-1,2,5-thiadiazol-4-yl-1,2,5,6-tetrahydro-1-methylpyridine
FCWAY	*N*-{2-[4-(2-methoxyphenyl)piperazinyl]ethyl}-*N*-(pyridin-2-yl) – fluorocyclohexanecarboxamide

PAC	Paclitaxel
P-gp	P-glycoprotein
CB-TE2A	4,11-bis(carboxymethyl)-1,4,8,1-tetraazabicyclo[6.6.2]hexadcane
TETA	1,4,8,11-tetraazacyclotetradecane-1,4,8,11-tetraacetic acid

References

1. Ter-Pogossian MM, Phelps ME, Hoffman EJ, Mullani NA. A positron-emission transaxial tomograph for nuclear imaging (PETT). Radiology. 1975; 114(1):89–98. [PubMed: 1208874]
2. Phelps ME, Hoffman EJ, Mullani NA, Ter-Pogossian MM. Application of annihilation coincidence detection to transaxial reconstruction tomography. J Nucl Med. 1975; 16(3):210–24. [PubMed: 1113170]
3. Fowler JS, Ido T. Initial and subsequent approach for the synthesis of 18FDG. Semin Nucl Med. 2002; 32(1):6–12. [PubMed: 11839070]
4. Giron MC, Portolan S, Bin A, Mazzi U, Cutler CS. Cyto-chrome P450 and radiopharmaceutical metabolism. Q J Nucl Med Mol Imaging. 2008; 52(3):254–66. [PubMed: 18475251]
5. Ma Y, Kiesewetter D, Lang L, Eckelman WC. Application of LC-MS to the analysis of new radiopharmaceuticals. Mol Imaging Biol. 2003; 5(6):397–403. [PubMed: 14667494]
6. Ma Y, Lang L, Kiesewetter D, Jagoda E, Eckelman WC. Species differences in metabolites of PET ligands: serotonergic 5-HT1A receptor antagonists 3-trans-FCWAY and 3-cis-FCWAY. Nucl Med Biol. 2006; 33(8):1013–9. [PubMed: 17127175]
7. Chu I, Nomeir AA. Utility of mass spectrometry for in-vitro ADME assays. Curr Drug Metab. 2006; 7(5):467–77. [PubMed: 16787156]
8. Korfmacher WA. Principles and applications of LC-MS in new drug discovery. Drug Discov Today. 2005; 10(20):1357–67. [PubMed: 16253874]
9. Lang L, Jagoda E, Ma Y, Sassaman MB, Eckelman WC. Synthesis and *in vivo* biodistribution of F-18 labeled 3-cis-, 3-trans-, 4-cis-, and 4-trans-fluorocyclohexane derivatives of WAY 100635. Bioorg Med Chem. 2006; 14(11):3737–48. [PubMed: 16488611]
10. Lang L, Jagoda E, Schmall B, Sassaman M, Ma Y, Eckelman WC. Fluoro analogs of WAY-100635 with varying pharmacokinetics properties. Nucl Med Biol. 2000; 27(5):457–62. [PubMed: 10962250]
11. Chay SH, Pohland RC. Comparison of quantitative whole-body autoradiographic and tissue dissection techniques in the evaluation of the tissue distribution of [14C]daptomycin in rats. J Pharm Sci. 1994; 83(9):1294–9. [PubMed: 7830246]
12. Yanes O, Woo HK, Northen TR, Oppenheimer SR, Shriver L, Apon J, Estrada MN, Potchoiba MJ, Steenwyk R, Manchester M, Siuzdak G. Nanostructure initiator mass spectrometry: tissue imaging and direct biofluid analysis. Anal Chem. 2009; 81(8):2969–75. [PubMed: 19301920]
13. Goodwin RJ, Pennington SR, Pitt AR. Protein and peptides in pictures: imaging with MALDI mass spectrometry. Proteomics. 2008; 8(18):3785–800. [PubMed: 18712772]
14. McCarron JA, Zoghbi SS, Shetty HU, Vermeulen ES, Wikstrom HV, Ichise M, Yasuno F, Halldin C, Innis RB, Pike VW. Synthesis and initial evaluation of [11C](R)-RWAY in monkey-a new, simply labeled antagonist radioligand for imaging brain 5-HT1A receptors with PET. Eur J Nucl Med Mol Imaging. 2007; 34(10):1670–82. [PubMed: 17579853]
15. Nelson DR. Cytochrome P450 and the individuality of species. Arch Biochem Biophys. 1999; 369(1):1–10. [PubMed: 10462435]
16. Lahoz A, Donato MT, Castell JV, Gomez-Lechon MJ. Strategies to *in vitro* assessment of major human CYP enzyme activities by using liquid chromatography tandem mass spectrometry. Curr Drug Metab. 2008; 9(1):12–9. [PubMed: 18220567]
17. Lahoz A, Donato MT, Montero S, Castell JV, Gomez-Lechon MJ. A new *in vitro* approach for the simultaneous determination of phase I and phase II enzymatic activities of human hepatocyte preparations. Rapid Commun Mass Spectrom. 2008; 22(2):240–4. [PubMed: 18088071]

18. Matusch A, Meyer PT, Bier D, Holschbach MH, Woitalla D, Elmenhorst D, Winz OH, Zilles K, Bauer A. Metabolism of the A1 adenosine receptor PET ligand [18F]CPFPX by CYP1A2: implications for bolus/infusion PET studies. Nucl Med Biol. 2006; 33(7):891–8. [PubMed: 17045169]

19. Ravasi L, Kiesewetter DO, Shimoji K, Lucignani G, Eckelman WC. Why does the agonist [(18)F]FP-TZTP bind preferentially to the M(2) muscarinic receptor? Eur J Nucl Med Mol Imaging. 2006; 33(3):292–300. [PubMed: 16333673]

20. Shimoji K, Esaki T, Itoh Y, Ravasi L, Cook M, Jehle J, Jagoda EM, Kiesewetter DO, Schmidt K, Sokoloff L, Eckelman WC. Inhibition of [18F]FP-TZTP binding by loading doses of muscarinic agonists P-TZTP or FP-TZTP *in vivo* is not due to agonist-induced reduction in cerebral blood flow. Synapse. 2003; 50(2):151–63. [PubMed: 12923818]

21. Jagoda EM, Kiesewetter DO, Shimoji K, Ravasi L, Yamada M, Gomeza J, Wess J, Eckelman WC. Regional brain uptake of the muscarinic ligand, [18F]FP-TZTP, is greatly decreased in M2 receptor knockout mice but not in M1, M3 and M4 receptor knockout mice. Neuropharmacology. 2003; 44(5):653–61. [PubMed: 12668051]

22. Kiesewetter DO, Vuong BK, Channing MA. The automated radiosynthesis of [18F]FP-TZTP. Nucl Med Biol. 2003; 30(1):73–7. [PubMed: 12493545]

23. Carson RE, Kiesewetter DO, Jagoda E, Der MG, Herscovitch P, Eckelman WC. Muscarinic cholinergic receptor measurements with [18F]FP-TZTP: control and competition studies. J Cereb Blood Flow Metab. 1998; 18(10):1130–42. [PubMed: 9778190]

24. Ma Y, Kiesewetter DO, Jagoda EM, Huang BX, Eckelman WC. Identification of metabolites of fluorine-18-labeled M2 muscarinic receptor agonist, 3-(3-[(3-fluoropropyl)thio]-1,2,5-thiadiazol-4-yl)-1,2,5,6-tetrahydro-1-methylpyridine, produced by human and rat hepatocytes. J Chromatogr B Analyt Technol Biomed Life Sci. 2002; 766(2):319–29.

25. Ma Y, Kiesewetter DO, Lang L, Der M, Huang B, Carson RE, Eckelman WC. Determination of [18F]FCWAY, [18F]FP-TZTP, and their metabolites in plasma using rapid and efficient liquid-liquid and solid phase extractions. Nucl Med Biol. 2003; 30(3):233–40. [PubMed: 12745014]

26. Kiesewetter DO, Jagoda EM, Shimoji K, Ma Y, Eckelman WC. Evaluation of [18F]fluoroxanomeline {5-{4-[(6-[18F]-fluorohexyl)oxy]-1,2,5-thiadiazol-3-yl}-1-methyl-1,2,3,6-tetrahydropyridine} in muscarinic knockout mice. Nucl Med Biol. 2007; 34(2):141–52. [PubMed: 17307122]

27. Murphy AT, Bonate PL, Kasper SC, Gillespie TA, De-Long AF. Determination of xanomeline in human plasma by ion-spray tandem mass spectrometry. Biol Mass Spectrom. 1994; 23(10):621–5. [PubMed: 7986832]

28. Murphy AT, Kasper SC, Gillespie TA, Delong AF. Determination of xanomeline and active metabolite, N-desmethylxanomeline, in human plasma by liquid chromatography-atmospheric pressure chemical ionization mass spectrometry. J Chromatogr B Biomed Appl. 1995; 668(2): 273–80. [PubMed: 7581862]

29. Cliffe IA. A retrospect on the discovery of WAY-100635 and the prospect for improved 5-HT(1A) receptor PET radioligands. Nucl Med Biol. 2000; 27(5):441–7. [PubMed: 10962248]

30. Pike VW, MJ, Hume SP, Ashworth S, Opacka-Juffry JSO. Pre-clinical development of a radioligand for studies of central 5-HT1A receptors *in vivo*-[11C]WAY-100635. Med Chem Res. 1994; 5:207–227.

31. Osman S, Lundkvist C, Pike VW, Halldin C, McCarron JA, Swahn CG, Farde L, Ginovart N, Luthra SK, Gunn RN, Bench CJ, Sargent PA, Grasby PM. Characterisation of the appearance of radioactive metabolites in monkey and human plasma from the 5-HT1A receptor radioligand, [carbonyl-11C]WAY-100635--explanation of high signal contrast in PET and an aid to biomathematical modelling. Nucl Med Biol. 1998; 25(3):215–23. [PubMed: 9620626]

32. Osman S, Lundkvist C, Pike VW, Halldin C, McCarron JA, Swahn CG, Ginovart N, Luthra SK, Bench CJ, Grasby PM, Wikstrom H, Barf T, Cliffe IA, Fletcher A, Farde L. Characterization of the radioactive metabolites of the 5-HT1A receptor radioligand, [O-methyl-11C]WAY-100635, in monkey and human plasma by HPLC: comparison of the behaviour of an identified radioactive metabolite with parent radioligand in monkey using PET. Nucl Med Biol. 1996; 23(5):627–34. [PubMed: 8905828]

33. Gallezot JD, Nabulsi N, Neumeister A, Planeta-Wilson B, Williams WA, Singhal T, Kim S, Maguire RP, McCarthy T, Frost JJ, Huang Y, Ding YS, Carson RE. Kinetic modeling of the serotonin 5-HT(1B) receptor radioligand [(11)C]P943 in humans. J Cereb Blood Flow Metab. 30(1):196–210. [PubMed: 19773803]
34. Zhang XY, Yasuno F, Zoghbi SS, Liow JS, Hong J, McCarron JA, Pike VW, Innis RB. Quantification of serotonin 5-HT1A receptors in humans with [11C](R)-(−)-RWAY: radiometabolite(s) likely confound brain measurements. Synapse. 2007; 61(7):469–77. [PubMed: 17415792]
35. Liow JS, Lu S, McCarron JA, Hong J, Musachio JL, Pike VW, Innis RB, Zoghbi SS. Effect of a P-glycoprotein inhibitor, Cyclosporin A, on the disposition in rodent brain and blood of the 5-HT1A receptor radioligand, [11C](R)-(−)-RWAY. Synapse. 2007; 61(2):96–105. [PubMed: 17117422]
36. Yasuno F, Zoghbi SS, McCarron JA, Hong J, Ichise M, Brown AK, Gladding RL, Bacher JD, Pike VW, Innis RB. Quantification of serotonin 5-HT1A receptors in monkey brain with [11C](R)-(−)-RWAY. Synapse. 2006; 60(7):510–20. [PubMed: 16952161]
37. Carson RE, Wu Y, Lang L, Ma Y, Der MG, Herscovitch P, Eckelman WC. Brain uptake of the acid metabolites of F-18-labeled WAY 100635 analogs. J Cereb Blood Flow Metab. 2003; 23(2): 249–60. [PubMed: 12571456]
38. Carson RE, Lang L, Watabe H, Der MG, Adams HR, Jagoda E, Herscovitch P, Eckelman WC. PET evaluation of [(18)F]FCWAY, an analog of the 5-HT(1A) receptor antagonist, WAY-100635. Nucl Med Biol. 2000; 27(5):493–7. [PubMed: 10962257]
39. Ma Y, Lang L, Kiesewetter DO, Jagoda E, Sassaman MB, Der M, Eckelman WC. Liquid chromatography-tandem mass spectrometry identification of metabolites of two 5-HT1A antagonists, N-[2-[4-(2-methoxylphenyl)piperazino]ethyl]-N-(2-pyridyl) trans- and cis-4-fluorocyclohexanecarboxamide, produced by human and rat hepatocytes. J Chromatogr B Biomed Sci Appl. 2001; 755(1–2):47–56. [PubMed: 11393732]
40. Bonne O, Bain E, Neumeister A, Nugent AC, Vythilingam M, Carson RE, Luckenbaugh DA, Eckelman W, Herscovitch P, Drevets WC, Charney DS. No change in serotonin type 1A receptor binding in patients with posttraumatic stress disorder. Am J Psychiatry. 2005; 162(2):383–5. [PubMed: 15677606]
41. Ma Y, Lang L, Kiesewetter DO, Eckelman WC. Liquid chromatography-tandem mass spectrometry identification of metabolites of three phenylcarboxyl derivatives of the 5-HT(1A) antagonist, N-(2-(4-(2-methoxyphenyl)-1-piperazinyl)ethyl)-N-(2-pyridyl) trans-4-fluorocyclohexanecarboxamide (FCWAY), produced by human and rat hepatocytes. J Chromatogr B Analyt Technol Biomed Life Sci. 2002; 780(1):99–110.
42. Horwitz SB. Mechanism of action of taxol. Trends Pharmacol Sci. 1992; 13(4):134–6. [PubMed: 1350385]
43. Kurdziel KA, Kiesewetter DO, Carson RE, Eckelman WC, Herscovitch P. Biodistribution, radiation dose estimates, and *in vivo* Pgp modulation studies of 18F-paclitaxel in nonhuman primates. J Nucl Med. 2003; 44(8):1330–9. [PubMed: 12902425]
44. Kiesewetter DO, Jagoda EM, Kao CH, Ma Y, Ravasi L, Shimoji K, Szajek LP, Eckelman WC. Fluoro-, bromo-, and iodopaclitaxel derivatives: synthesis and biological evaluation. Nucl Med Biol. 2003; 30(1):11–24. [PubMed: 12493538]
45. Boswell CA, McQuade P, Weisman GR, Wong EH, Anderson CJ. Optimization of labeling and metabolite analysis of copper-64-labeled azamacrocyclic chelators by radio-LC-MS. Nucl Med Biol. 2005; 32(1):29–38. [PubMed: 15691659]
46. Verduyckt T, Kieffer D, Huyghe D, Cleynhens B, Verbeke K, Verbruggen A, Bormans G. Identity confirmation of 99mTc-MAG3, 99mTc-sestamibi and 99mTc-ECD using radio-LC-MS. J Pharm Biomed Anal. 2003; 32(4–5):669–78. [PubMed: 12899957]
47. Liu S, Ziegler MC, Edwards DS. Radio-LC-MS for the characterization of 99mTc-labeled bioconjugates. Bioconjug Chem. 2000; 11(1):113–7. [PubMed: 10639093]
48. Vanderghinste D, Van Eeckhoudt M, Terwinghe C, Mortelmans L, Bormans GM, Verbruggen AM, Vanbilloen HP. An efficient HPLC method for the analysis of isomeric purity of technetium-99mexametazime and identity confirmation using LC-MS. J Pharm Biomed Anal. 2003; 32(4–5):679–85. [PubMed: 12899958]

49. Ma Y, Lang L, Reyes L, Tokugawa J, Jagoda EM, Kiesewetter DO. Application of highly sensitive UPLC-MS to determine biodistribution at tracer doses: validation with the 5-HT1A ligand [(18)F]FPWAY. Nucl Med Biol. 2009; 36(4):389–93. [PubMed: 19423006]

50. Chernet E, Martin LJ, Li D, Need AB, Barth VN, Rash KS, Phebus LA. Use of LC/MS to assess brain tracer distribution in preclinical, *in vivo* receptor occupancy studies: dopamine D2, serotonin 2A and NK-1 receptors as examples. Life Sci. 2005; 78(4):340–6. [PubMed: 16139310]

51. Barth VN, Chernet E, Martin LJ, Need AB, Rash KS, Morin M, Phebus LA. Comparison of rat dopamine D2 receptor occupancy for a series of antipsychotic drugs measured using radiolabeled or nonlabeled raclopride tracer. Life Sci. 2006; 78(26):3007–12. [PubMed: 16434058]

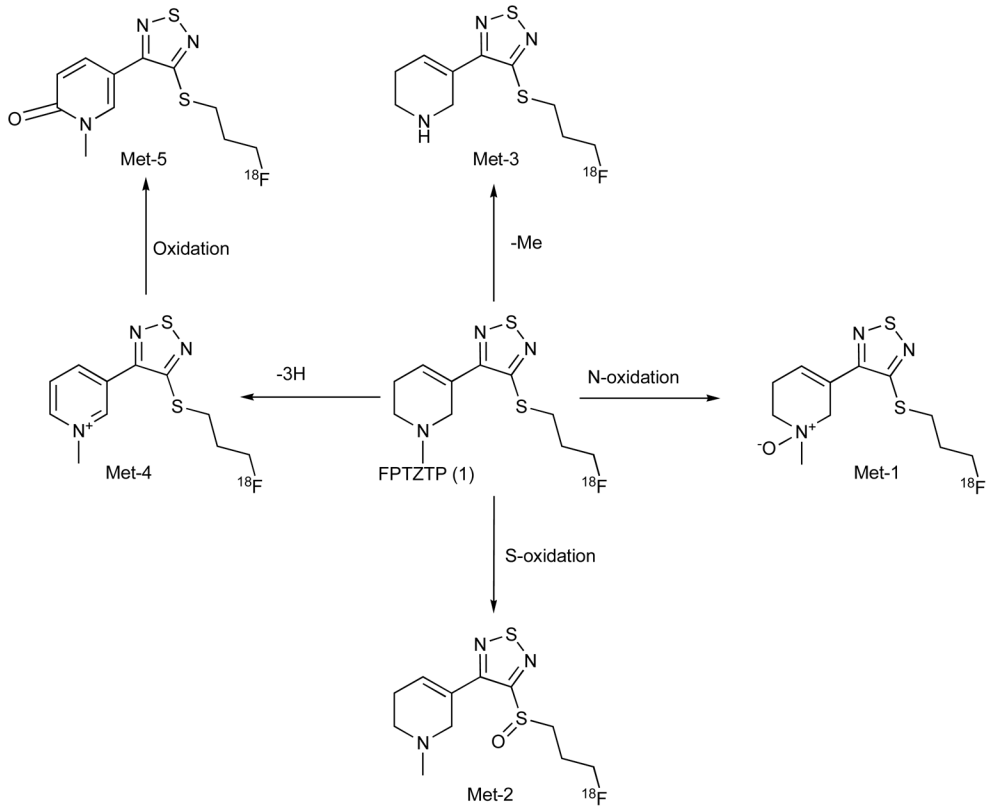

Fig. 1.

In vitro metabolites of FP-TZTP upon incubation with hepatocytes (rat, monkey, and human). Structures were determined by LC/MS/MS and compared with synthesized standards. There were no significant species differences in the metabolite profile.

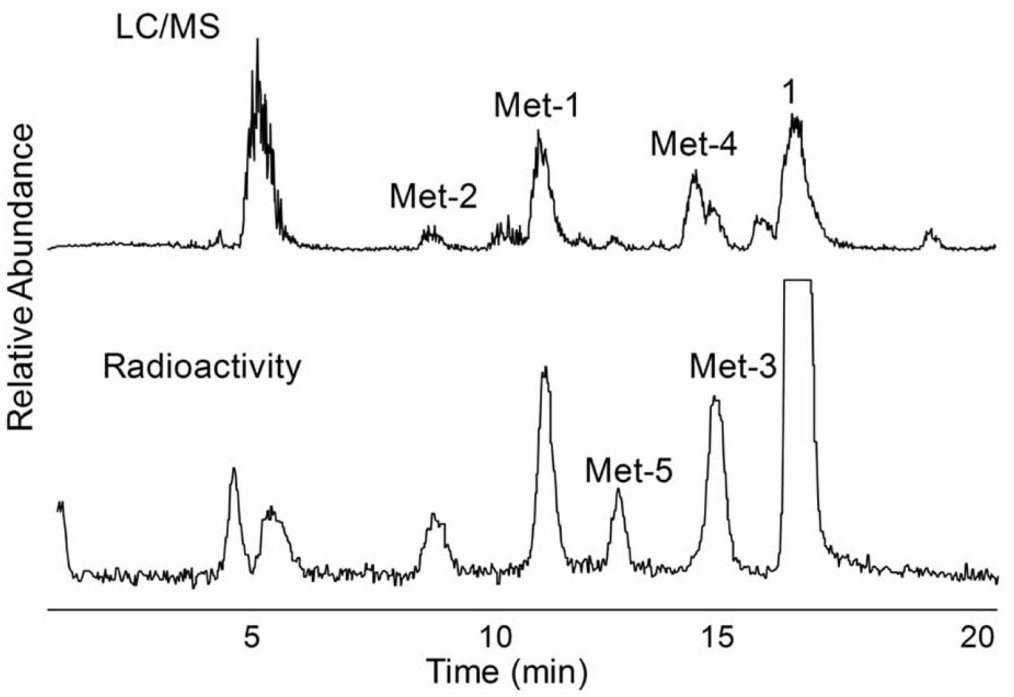

Fig. 2.

Chromatograms of carrier-added ^{18}F-FP-TZTP metabolites produced by 2-h incubation using cryopreserved human hepatocytes. HPLC elution was monitored by online radioactivity detector and ESI-MS. Top: MS TIC; bottom: on-line radioactivity.

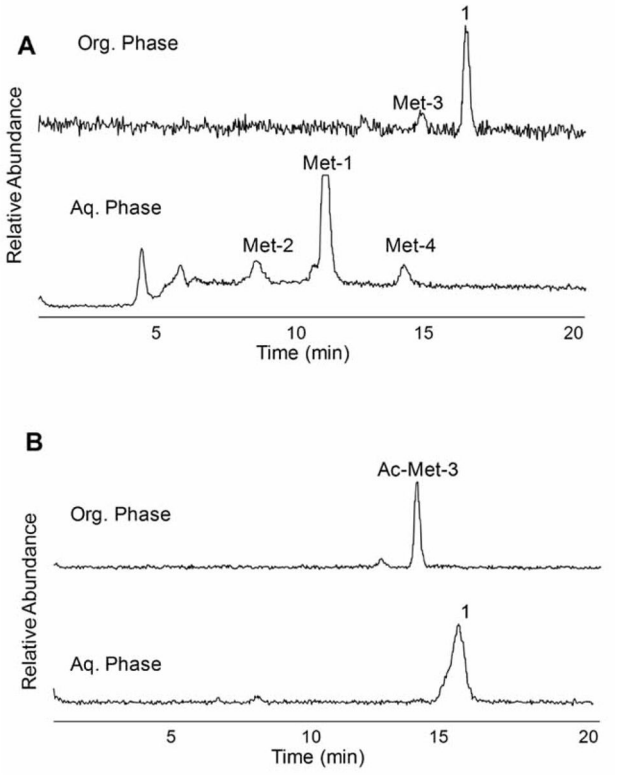

Fig. 3.

Quantitative extraction of parent FP-TZTP from its metabolites in plasma by a two-step two-phase solvent system. (A) Radio-HPLC chromatograms of organic and aqueous phases of **(A)** first extraction and **(B)** second extraction. The peaks are labeled with the proposed structure.

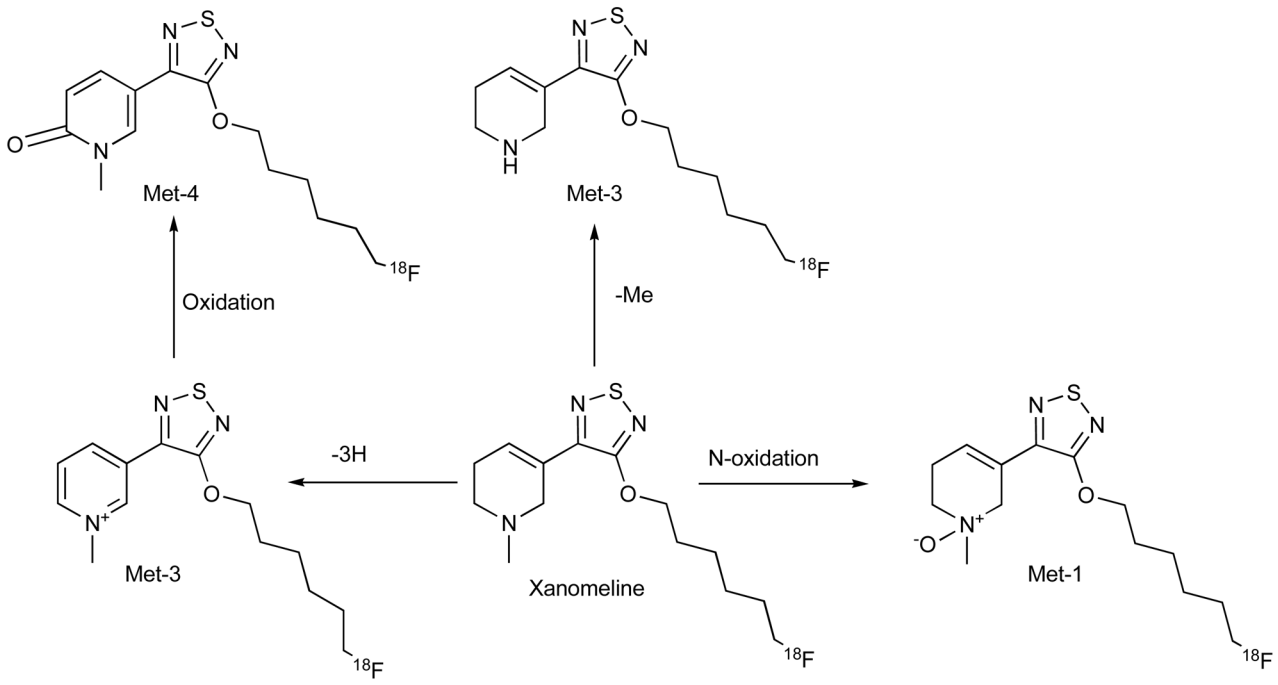

Fig. 4.

In vitro metabolites of fluoro xanomeline upon incubation with hepatocytes (rat, monkey, and human). Structures were determined by LC/MS/MS and compared with synthesized standards. There were no significant species differences in the metabolite profile.

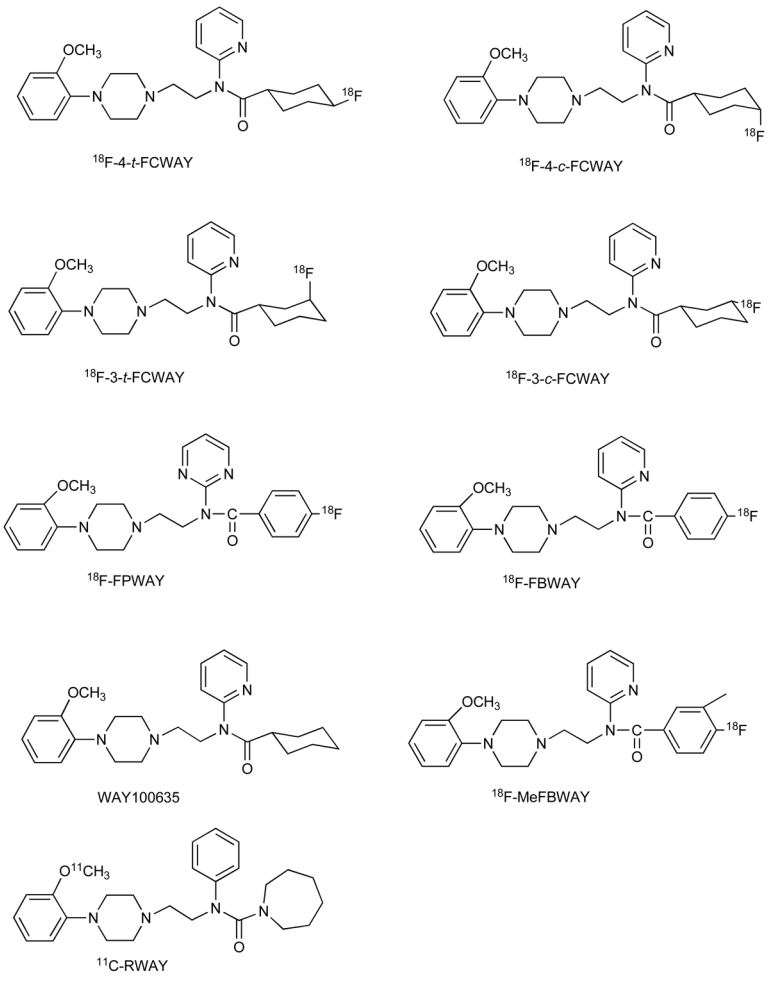

Fig. 5.
Structures of 5-HT_{1A} receptor ligands and related compounds

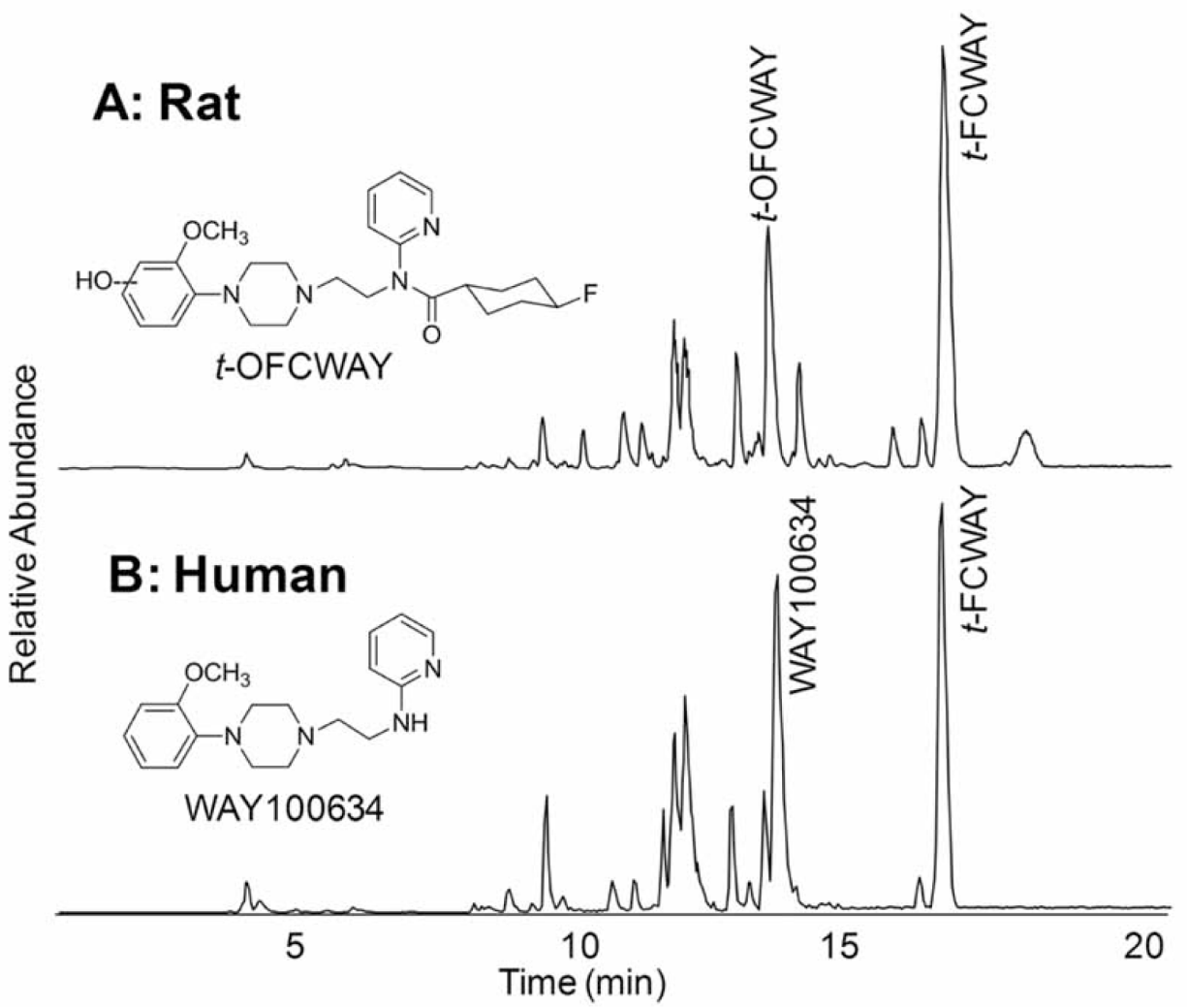

Fig. 6.

LC/MS chromatogram of *t*-4-FCWAY metabolites produced by 2-h incubation using cryopreserved rat **(A)** and human **(B)** hepatocytes. Structures were determinate by LC/MS/MS and compared with synthesized standards. *t*-OFCWAY was the major metabolite of rat hepatocytes and WAY100634 was the major metabolite of human hepatocytes.

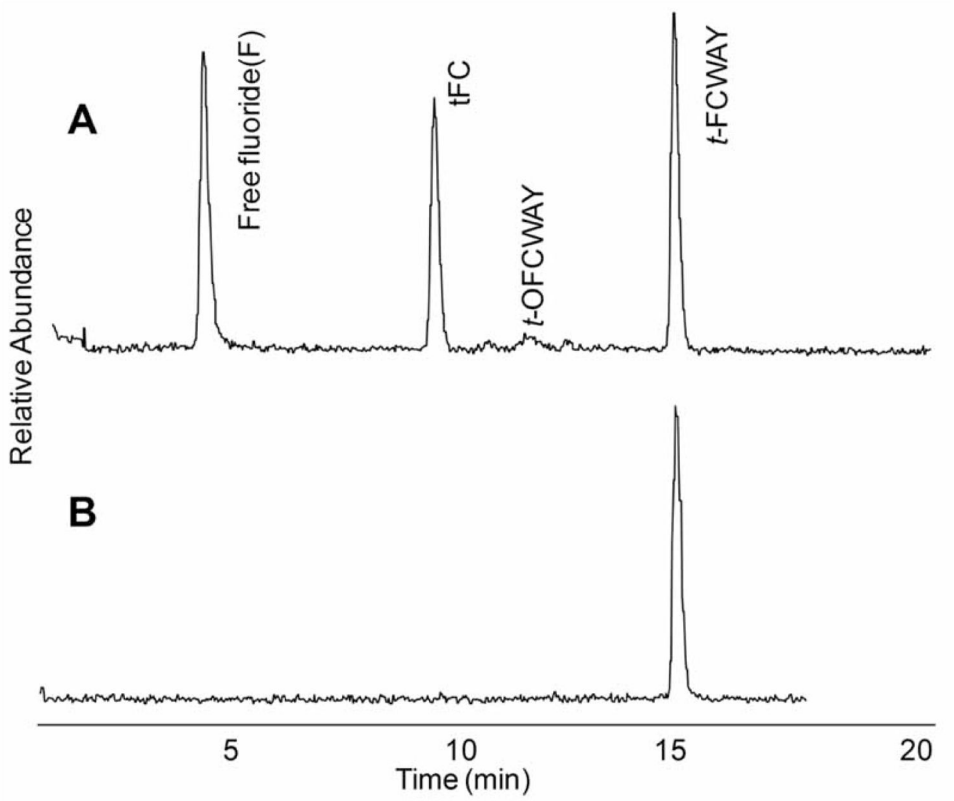

Fig. 7.

(A) Radiochromatogram of carrier-added ^{18}F-*t*-4-FCWAY metabolites after incubation with human hepatocytes. Free fluoride and FC (4-trans-fluorocyclohexanecarboxylic acid) were the major radiolabeled metabolites. **(B)** ^{18}F-*t*-4-FCWAY standard.

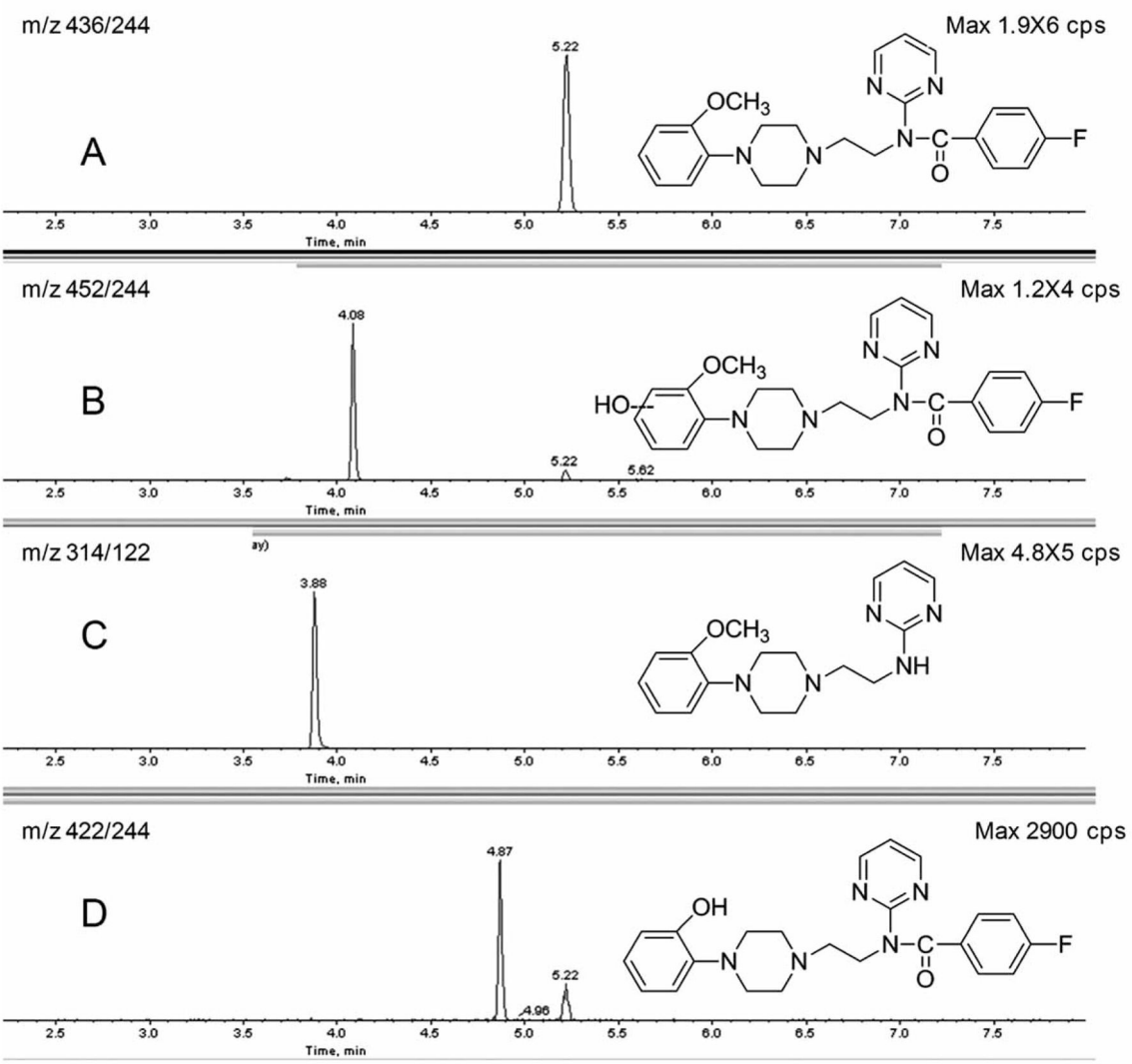

Fig. 8.

The metabolites of FPWAY in brain extract after intravenous administration with FPWAY (110 nmol) and sacrificed after 30 min. The brains were removed and extracted with acetonitrile (1:1; g:ml). The identities of the metabolites were determined by MRM of parent compound (A: m/z 436/244), oxidation (B: m/z452/244), amide hydrolysis metabolites (C: m/z 314/122), and demethylation (D: m/z 422/244).

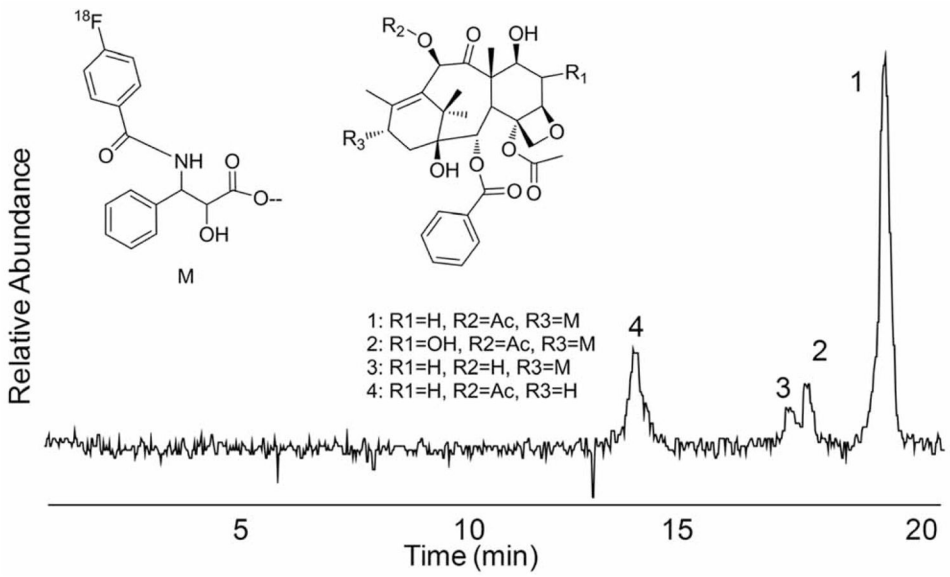

Fig. 9.
Radiochromatogram of ^{18}F-Paclitaxel metabolites from rat hepatocytes.

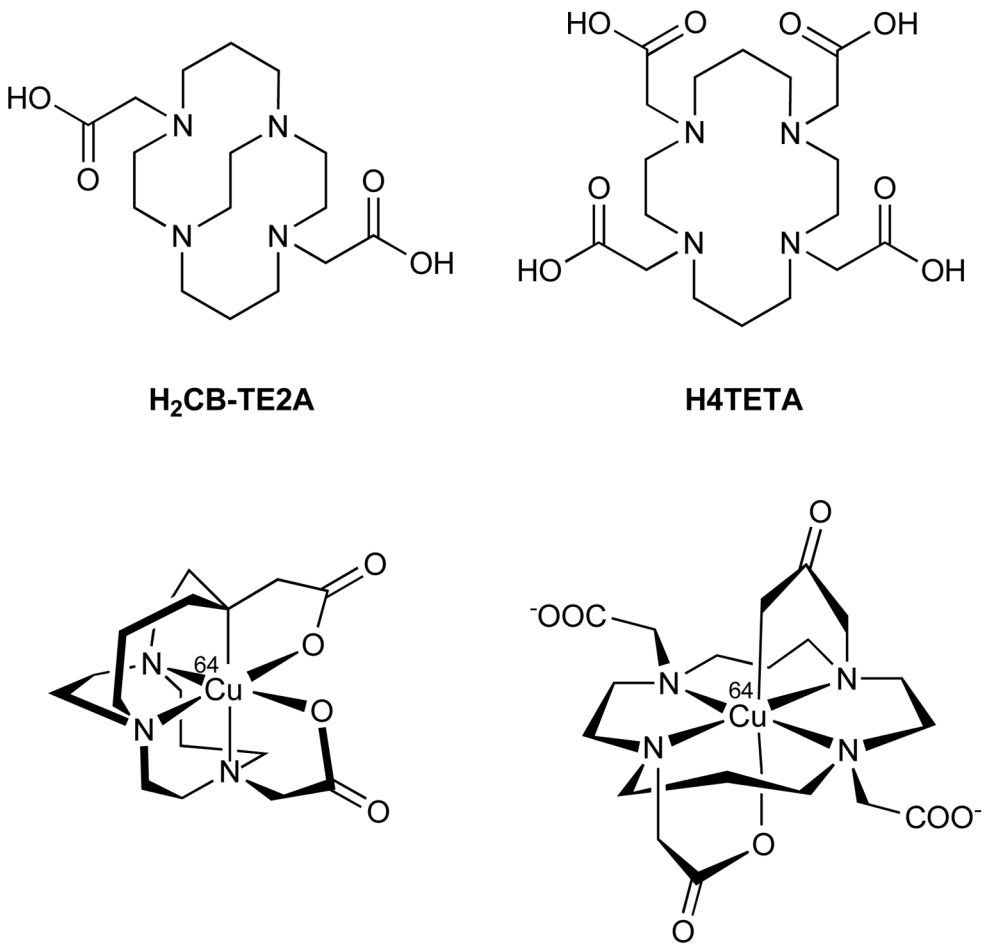

Fig. 10.

Structural comparison of H_2CB-TE2A, H_4TETA (top), and structural representations of the corresponding ^{64}Cu-labeled complexes based on solved crystal structures.

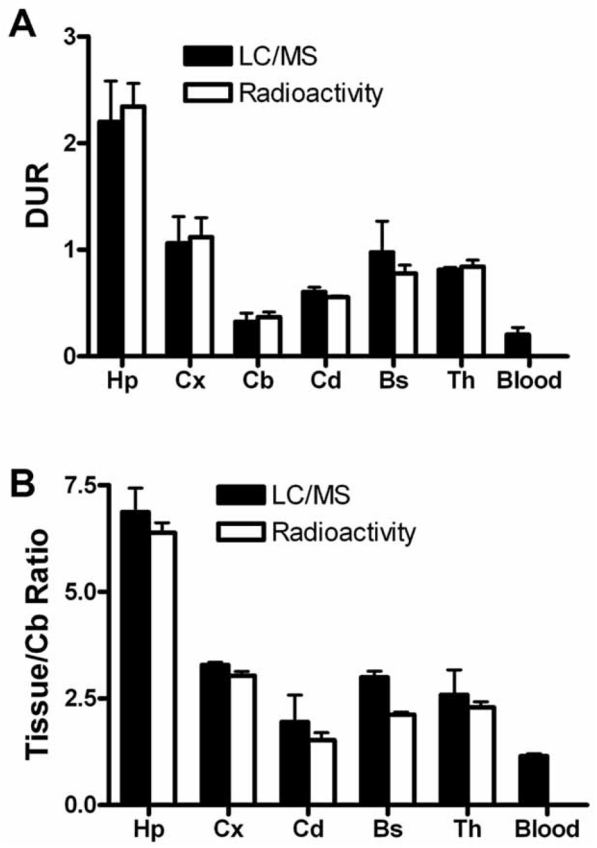

Fig. 11.

The biodistribution studies of [^{18}F]FPWAY. The six regions of rat brain [hippocampus (Hp), cortex (Cx), cerebellum (Cb), caudate (Cd), brain stem (BS), and thalamus (Th)] and plasma (P) were processed for quantitative measurement of parent compound concentration by LC-MS. The data (black bar) were then converted to **(A)** the differential uptake ratio DUR (%ID/g × body weight/100) and **(B)** the brain tissue-specific binding ratio [(DUR_{tissue}/$DUR_{cerebellum}$) − 1] to allow direct comparison with data (white bar) obtained by gamma counting of the coinjected radioactive [^{18}F]FPWAY. The DUR and the brain tissue-specific binding ratio calculated using the LC-MS method were highly correlated to the values obtained by standard radioactivity measurements of [^{18}F]FPWAY.